Heliyon 10 (2024) e31444

Contents lists available at ScienceDirect

Heliyon

journal homepage: www.cell.com/heliyon

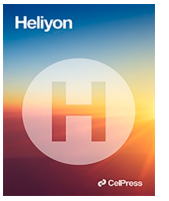

Research article

A GAD1 inhibitor suppresses osteosarcoma growth through the Wnt/β-catenin signaling pathway

Changchun Jian [a,b], Ben Wang [a,b], Hai Mou [a,b], Ye Zhang [a,b], Chaohua Yang [a,b], Qiu Huang [a,b], Yunsheng Ou [a,b,*]

[a] *Department of Orthopedics, The First Affiliated Hospital of Chongqing Medical University, Chongqing, 400016, China*
[b] *Orthopedic Laboratory of Chongqing Medical University, Chongqing, 400016, China*

ARTICLE INFO

Keywords:
Glutamate acid decarboxylase 1
β-catenin
3-Mercaptopropionic acid
Growth
Osteosarcoma

ABSTRACT

Background: As a marker of the GABAergic system, the expression of glutamate decarboxylase 1 (GAD1) is mainly restricted to the central nervous system. Emerging studies have shown that aberrant expression of GAD1 in tumor tissues may promote tumor cell growth. The role of GAD1 in the development of osteosarcoma (OS) remains unclear, so this study sought to investigate the expression status of GAD1 and the effect of its specific inhibitor 3-mercaptopropionic acid (3-MPA) on OS.

Methods: The R2 database was used to analyze the relationship between the expression of GAD1 and clinical prognosis in OS patients. Immunohistochemistry was used to compare the expression profile of GAD1 between OS and matched neighboring tissues. The potential antitumor effects of 3-MPA on cell viability, colony formation and the cell cycle were examined. Moreover, the in vivo effect of 3-MPA on tumor growth was investigated using tumor-bearing nude mice.

Results: The expression level of GAD1 was aberrantly upregulated in OS tissues, but almost no expression of GAD1 was found in matched neighboring tissues. Western blotting analyses showed upregulation of GAD1 in OS cells compared to human osteoblast cells. In vitro and in vivo, 3-MPA significantly suppressed the growth of OS. Regarding the mechanism, 3-MPA inhibited β-catenin and cyclin D1 in OS cells, thereby inactivating the Wnt/β-catenin pathway.

Conclusions: OS displays increased expression of the GABAergic neuronal marker GAD1, and 3-MPA significantly reduces OS growth by inhibiting the Wnt/β-catenin pathway.

1. Introduction

Osteosarcoma (OS) is the most prevalent primary malignant bone tumor, yet its underlying mechanism is mostly unknown [1]. Although numerous therapeutic approaches, such as surgical methods, neoadjuvant chemotherapy and immunotherapy drugs, are used to treat OS, the survival rate has remained the same over the past 30 years [2]. With current developments in the genetic characterization of OS, it is critical to discover novel biomarkers to facilitate the development of therapeutic strategies.

Tumor growth and dissemination are strongly associated with the localized microenvironment [3], which consists of tumor, stromal, vascular and immune cells. Many types of nerves are present in the tumor microenvironment (TME), and increasing evidence has revealed that the nervous system has a crucial function in tumor initiation and progression [4,5]. Neural density and neuronal

* Corresponding author. Department of Orthopedics, The First Affiliated Hospital of Chongqing Medical University, Chongqing, 400016, China.
E-mail address: ouyunsheng2001@163.com (Y. Ou).

https://doi.org/10.1016/j.heliyon.2024.e31444
Received 18 May 2023; Received in revised form 15 May 2024; Accepted 15 May 2024
Available online 17 May 2024

biomarkers of the TME appear to be crucial diagnostic and prognostic markers in various tumors [4]. Nerve-derived neurotransmitters can control the growth of a variety of cancers, such as breast, pancreatic, gastric, prostate and other cancers [6–8]. Elucidation of tumor-nerve cell interactions in the TME could provide new treatment options. The regulation of neuronal signaling could represent a new treatment approach targeting the entire TME [5].

Intriguingly, some tumor cells display an increased neuron-like gene signature [9,10], and lung, colorectal [11] and pancreatic cancers [12] were found aberrant expression of the GABAergic neuronal marker glutamate decarboxylase 1 (GAD1). Originally, the expression of GAD1, which is among the two GAD isoforms essential for γ-aminobutyric acid (GABA) production, was believed to be mainly restricted to the central nervous system (CNS) [11,13]. Under physiological conditions, GABA is an important inhibitory neurotransmitter in the CNS. However, emerging studies support a role for GABA beyond conventional neurotransmission as a strong agent controlling tumor cell proliferation and metastasis [13]. GABA-positive tumors usually express GAD1, and elevated GAD1 expression in tumors is often associated with increased proliferative and/or invasive potential [11,12,14,15].

Numerous studies have suggested that the precise targeting of nerve-tumor interactions may provide new opportunities to improve the prognosis of many difficult-to-treat malignancies [16], and targeting GAD1 has been shown to be an effective therapeutic approach in various tumors [11,15]. Nevertheless, the function of GAD1 in OS growth and progression remains unclear. Our goal was to determine GAD1 expression status in OS and to evaluate the effects of its specific inhibitor, 3-mercaptopropionic acid (3-MPA), on the growth of OS cells.

2. Materials and methods

2.1. Clinical samples

Paraffin-embedded specimens and matched neighboring tissues of patients with OS were acquired from the First Affiliated Hospital of Chongqing Medical University. The use of human specimens in this survey was approved by the Ethics Committee of the First Affiliated Hospital of Chongqing Medical University. Every patient signed permission forms requiring informed consent. Immunohistochemistry (IHC) analysis with an anti-GAD1 antibody (Bioss, China, bs-1302R) was used to determine the GAD1 expression levels. In addition, we used the public dataset for OS (https://hgserver1.amc.nl/cgi-bin/r2/main.cgi. Retrieved December 5, 2022) containing 127 OS samples to analyze the level of GAD1 in OS patients.

2.2. Cell lines and reagents

HOS, MG-63, and 143B human OS cell lines were purchased from Procell Life Science and Technology (Hunan, China). hFoB1.19 cells were purchased from Bluefbio (Shanghai) Biology Technology Development Co., Ltd. (Shanghai, China). Saos-2 and U2-OS cells were purchased from iCell Bioscience Inc. (Shanghai, China). SJSA-1 cells were purchased from Fenghui Biotechnology Co., Ltd. (Hunan, China). A 37 °C incubator with 5 % CO2 and humidified air was used to cultivate the cells in DMEM with 10 % fetal bovine serum (FBS) and penicillin/streptomycin. The inhibitor 3-MPA with over 99 % purity 3-MPA was purchased from Sigma–Aldrich.

2.3. Cell viability assay

An APExBio cell counting kit (CCK-8; Houston, TX, USA) was used to determine the viability of HOS and MG-63 cells. A total of 2000 cells/well were plated in 96-well microplates and cultivated overnight. The cells were subsequently treated with 3-MPA at various doses for 24, 48, and 72 h in an incubator. Every well received 10 μL of CCK-8 solution, followed by incubating the cells for an additional 3 h at 37 °C in the dark, and then, the optical density (OD) was evaluated at 450 nm. Based on the following formula, cell viability (%) was calculated as follows: study OD/control OD × 100 %. Each experiment was conducted in triplicate.

2.4. Colony formation assay

On a six-well plate, approximately 500 HOS and MG-63 cells were plated. After 24 h, the cells were treated with 7.5 μM and 10 μM 3-MPA. Following treatment with 3-MPA for 48 h, fresh medium was added to all wells and incubated for 8–10 days or until considerably larger colonies were detected in the control group. 4 % paraformaldehyde (Beyotime) was utilized for the fixation of the colonies before applying the crystal violet stain. ImageJ software was used to quantify the colonies, and Prism 9.4.1 software was used to plot them. There were at least three repetitions of each experiment.

2.5. Transwell assay

OS cells were suspended in serum-free Dulbecco's modified Eagle's medium (DMEM) and seeded into Transwell chambers (8 mm, Corning, USA) at a concentration of 3×10^5 cells/ml. For invasion assays, the chambers were precoated with 1:8 diluted Matrigel (Corning, USA), while migration assays were performed without coating. The lower chamber of a 24-well plate was filled with DMEM containing 15 % fetal bovine serum, and the cells were incubated for 16 h for migration assays and 24 h for invasion assays. After incubation in a 37 °C, 5 % CO2 incubator, the chambers were removed, and the Matrigel and cells in the upper chamber were carefully wiped off using a cotton swab. The cells were fixed with 4 % paraformaldehyde (Beyotime) for 15 min, stained with 0.1 % crystal violet (Beyotime) for 15 min, and counted using an Olympus upright light microscope.

2.6. EdU (5-ethynyl-2′-deoxyuridine) assay in vivo

The thymidine nucleotide analog EdU was utilized for the in vivo marking of dividing cell nuclei, and an EdU test kit (Beyotime Biotechnology) was used. Both groups of mice received an intraperitoneal injection of EdU (50 mg kg^{-1} body weight) [17] on day 27, 72 h before sacrifice. The proportion of EdU-positive cells was measured utilizing a fluorescence scanner.

2.7. Cell cycle analysis using flow cytometry

The cell cycle was examined using a flow cytometric technique. Briefly, following 48 h of treatment with 10 μM 3-MPA, HOS and MG-63 cells were trypsinized, washed twice and then fixed with 75 % ethanol at 4 °C for 48 h. A FACScan system (BD Biosciences, USA) was used to determine the cell cycle distribution in fixed cells.

2.8. Western blotting

A suitable density of OS cells was seeded in a Petri dish. Following incubation for 24 h, the cells were subjected to 48 h of treatment with 0, 2.5, 5, 7.5, and 10 μM 3-MPA. The cells were collected after 48 h, and total protein was recovered using RIPA cell lysate (Beyotime, China). A BCA kit (Beyotime) was used to determine the concentration of protein. A 10 % SDS–PAGE (EpiZyme, China) was used to separate equivalent amounts of protein from every sample, which were then transferred to PVDF membranes and blocked with 5 % nonfat milk for 1.5 h at room temperature. Afterward, the following primary antibodies were applied and incubated overnight at 4 °C: anti-GAD67 (1:1000; Abmart, China, TU337771), anti-Cyclin D1 (1:1000; Abmart, T55404), anti-β-catenin (1:1000; Abmart, M24002) and anti-GAPDH (1:4000; Bioss, China, bs-0755R). Secondary antibodies were then probed for 1 h at room temperature on the blots. For analysis of the protein bands, a chemiluminescence imaging system (Bio-Rad, USA) was used with an electrochemiluminescence detection kit (Zenbio, China, 17047). ImageJ was used to analyze densitometric data on protein bands.

2.9. Hematoxylin–eosin (H&E) and IHC

Mice with xenograft tumors were sacrificed to collect and fix their tissues with 4 % paraformaldehyde for histopathological investigation. An ethanol gradient and xylene were used to dry the tumor tissues before paraffin embedding and sectioning at 4 mm thickness. IHC was utilized to evaluate β-catenin and Ki67 expression. Tumor sections were blocked and stained with antibodies targeting β-catenin (1:200) and Ki67 (1:200). Paraffin-embedded specimens and matched adjacent tissues of patients with OS were stained with H&E and GAD1 expression in these tissues was determined using IHC. Finally, images were taken utilizing a microscope, and the count of cells positive for the target proteins was measured in five randomized fields at 200 × magnification using a light microscope. The data are presented as a proportion of positive cells or an average optical density value.

2.10. Subcutaneous xenograft model

The Ethics Committee of the First Affiliated Hospital of Chongqing Medical University approved each animal experiment. Beijing Huafukang Biotechnology Co., Ltd., supplied approximately nude female BALB/c mice aged four weeks. For acclimatization, the mice were housed for nearly a week with easy accessibility to a commercial meal and water in particular circumstances free from pathogens. Subcutaneous injections of 100 μL of PBS with $1x10^6$ HOS cells were used to develop tumor-bearing mice. In groups of 5 each, mice were randomly assigned to treatment and control groups as soon as the tumor volume reached 50 mm^3. Then, vehicle (saline) or 3-MPA (15 mg kg^{-1}) was intratumorally injected every day [11] in the control group or the treatment group, respectively. A three-day interval was used to measure tumor sizes. Each mouse was weighed every 6 days, and tumor volumes were calculated using the following formula: $1/2\ a^2\ b$ (where a is the short axis, and b is the long axis). On day 30, the experiment ended, and the mice were euthanized, followed by weighing and evaluating their tumors. The excised tumors were fixed in 4 % paraformaldehyde for ex vivo analysis.

2.11. Statistical analysis

The statistical analysis was conducted using GraphPad Prism software. The data are expressed as the mean ± standard deviation (SD) and were analyzed using either Student's t-test or one-way ANOVA. The analyses were based on triplicate experimental data, and the significance levels were indicated as $*p < 0.05$, $**p < 0.01$, and $***p < 0.001$.

3. Results

3.1. GAD1 overexpression in OS patients is related to poor prognosis

We used the R2 public database to analyze data from the GEO database (GSE42352). Kaplan–Meier curve analysis indicated that elevated GAD1 expression results in reduced survival of OS patients (Fig. 1A). GAD1 expression was significantly greater in OS cells than in normal bone cells (Fig. 1B). In total, 48 tumor and matching adjacent tissue specimens from OS patients were collected. Our results revealed that the OS tissues showed elevated expression levels of GAD1, but no staining was observed in the adjacent

nontumorous tissues (Fig. 1C). For experimental investigations, we evaluated GAD1 levels in the human osteoblast cell line hFoB1.19 and OS cell lines and found that all OS-derived cell lines had significantly higher GAD1 protein expression than the hFoB1.19 cell line (Fig. 1D–E). Together, the correlation between GAD1 upregulation and poor prognosis suggests that GAD1 has a tumorigenic function in OS patients.

3.2. *Treatment with 3-MPA inhibits the growth and colony-forming ability and induces cell cycle arrest of OS cells*

HOS and MG-63 cells were exposed to 3-MPA with different concentrations and durations to evaluate its antiproliferative effects. OS cell viability was examined, and 3-MPA was shown to strongly inhibit OS cell growth. The half maximal inhibitory concentration (IC50) values of 3-MPA were 9.05 and 9.26 μM at 48 h and 7.44 and 7.45 μM at 72 h (Fig. 2A–B). The results of colony formation assays indicated that 7.5 μM 3-MPA decreased colony formation by approximately 30 %, whereas 10 μM 3-MPA decreased colony formation by approximately 90 % in both cell lines. These findings revealed that 3-MPA has growth-suppressive effects on OS cells (Fig. 2C–D). We also examined the cell cycle status of OS cells after 48 h of treatment with 10 μM 3-MPA. The proportion of OS cells in the G1 phase was elevated, whereas the proportion of OS cells in the S and G2 phases was reduced (Fig. 2E–H). Our findings revealed that 3-MPA has growth-suppressive effects on OS cells.

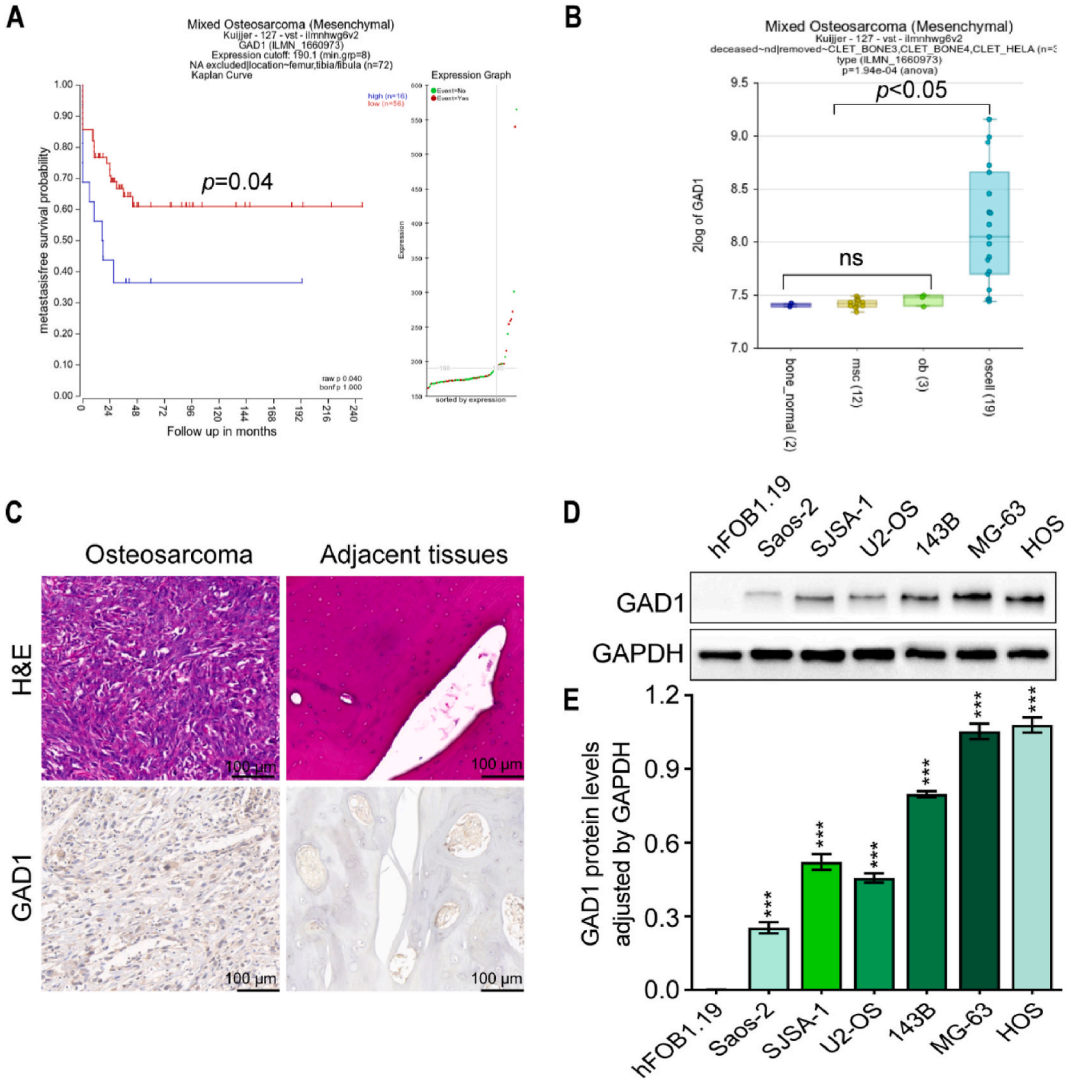

Fig. 1. GAD1 overexpression is related to a poor prognosis for OS patients. (A) Metastasis-free survival (MFS) results for 16 and 56 patients with elevated and decreased GAD1 expression, respectively; (B) Expression levels of GAD1 in normal bone and OS cell lines; (C) IHC staining showing GAD1 expression levels in human OS specimens and matched neighboring tissues. Scale bars, 100 μm; (D–E) Western blotting was performed to determine GAD1 levels in OS cell lines and hFoB1.19 cells. ***$p < 0.001$; NS, not significant.

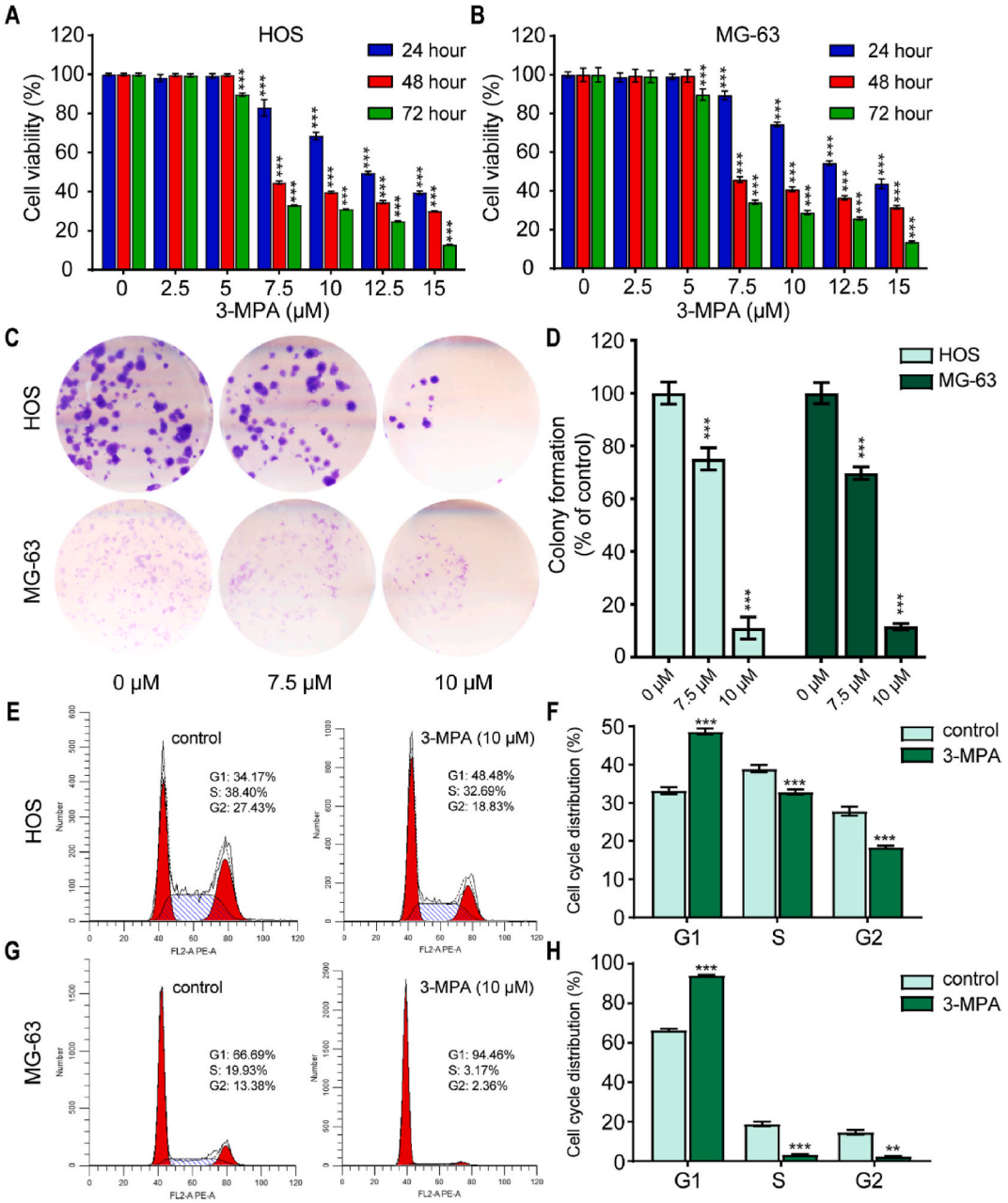

Fig. 2. Treatment with 3-MPA suppresses OS cell growth by stimulating cell cycle arrest. (A–B) HOS and MG-63 cells were subjected to various doses of 3-MPA, and then, the effects of 3-MPA on cell growth were evaluated utilizing CCK-8 assays at 24, 48 and 72 h. (C–D) Treatment with 7.5 and 10 μM 3-MPA was performed to measure the anti-clonogenic impacts of 3-MPA. (E–H) Two OS cell lines were treated with 10 μM 3-MPA for 48 h before being collected and analyzed for cell cycle advancement. $^{**}p < 0.01$, $^{***}p < 0.001$.

3.3. Treatment with 3-MPA has no effect on the migration and invasion of OS cells

We also assessed the effects of 3-MPA on the migration and invasion of OS cells through transwell assays. Unfortunately, our results indicated that 3-MPA had no significant impact on the migration and invasion capabilities of OS cells (Fig. 3A–D). Additionally, we examined the expression of epithelial–mesenchymal transition (EMT) proteins after 3-MPA treatment, and the results showed that 3-MPA did not affect the expression of EMT proteins in OS cells (Fig. 3E–G).

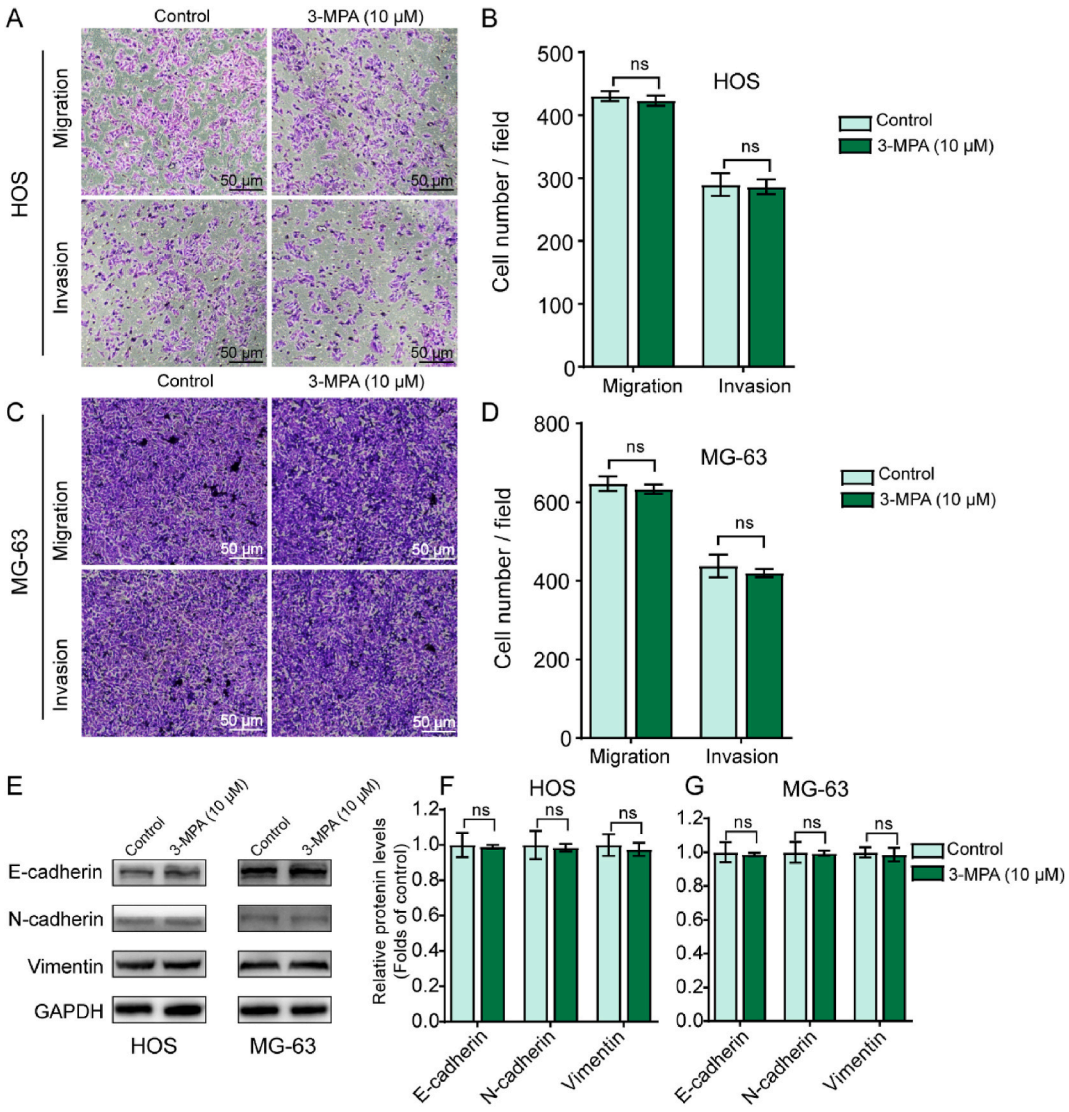

Fig. 3. Treatment with 3-MPA did not alter the motility of OS cells. (A–D) Transwell assays were utilized to evaluate the impact of 3-MPA on the migration and invasion abilities of OS cells. Scale bars, 50 μm. (E–G) Western blotting was used to detect the levels of E-cadherin, N-cadherin and Vimentin proteins in OS cells with or without the use of 3-MPA. NS, not significant.

3.4. Suppression of Wnt/β-catenin signaling by 3-MPA treatment in OS cells

To determine the mechanism by which 3-MPA inhibits cell proliferation, we performed western blotting of HOS and MG-63 cells treated with the control (0 μM) and different concentrations of 3-MPA. Since β-catenin signaling is known to be oncogenic in many cases [18] and the inhibitory effect of 3-MPA on β-catenin signaling has been demonstrated in oral cancer [15], lung cancer and colorectal adenocarcinoma [11], we hypothesize that 3-MPA may also exert its inhibitory effects on OS proliferation through this pathway. Consistent with previous research, our findings indicated that 3-MPA suppressed β-catenin expression in a concentration-dependent manner (Fig. 4A–B, 4D-E). Moreover, the expression of cyclin D1, a cell cycle protein that induces G1 development and a direct target gene of β-catenin, was also blocked by 3-MPA treatment (Fig. 4A, C; D, F).

3.5. Treatment with 3-MPA inhibits OS growth in vivo

Nude BALB/c mice were implanted with HOS cells subcutaneously into the right flank to determine the in vivo effectiveness of 3-MPA. Our results indicated that 3-MPA treatment significantly decreased tumor growth compared with that of the control group (Fig. 5A–C). Additionally, daily intratumoral injection of 3-MPA did not alter mouse weight (Fig. 5D), suggesting that the antitumor dose of 3-MPA (15 mg kg^{-1}) utilized in our trials was safe and showed no overall toxicity. The EdU assay showed that the

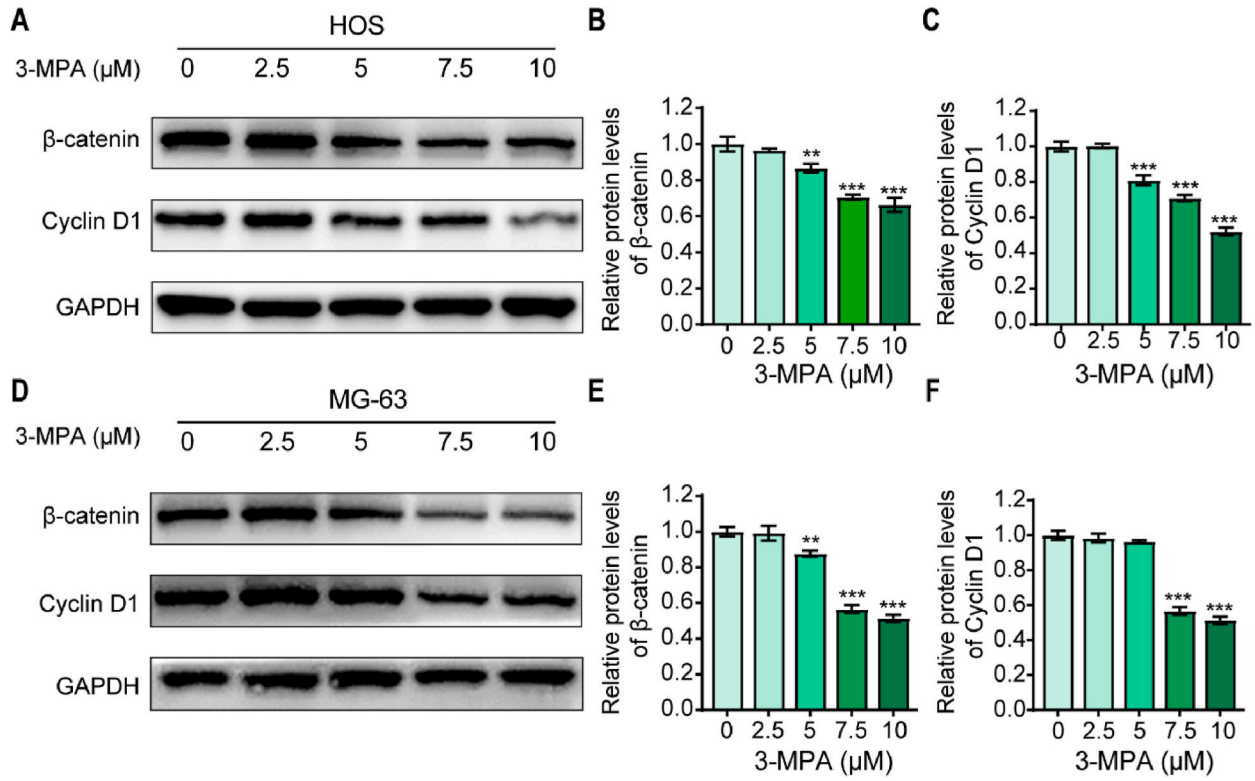

Fig. 4. Treatment with 3-MPA suppressed Wnt/β-catenin signaling in OS cells. (A–C) The protein levels of β-catenin and cyclin D1 in HOS cells treated with 3-MPA (0, 2.5, 5, 7.5 and 10 μM) in an incubator for 48 h. (D–F) Western blotting to evaluate the impact of various doses of 3-MPA on β-catenin and cyclin D1 in MG-63 cells. $^{**}p < 0.01$, $^{***}p < 0.001$.

administration of 3-MPA significantly suppressed tumor proliferation (Fig. 5E–F). We assessed the expression of the growth marker Ki67 to further verify the antitumor growth effects of 3-MPA treatment. Ki67 expression levels in tumor samples evaluated using IHC were decreased in the 3-MPA-treated group compared with the control group (Fig. 5G). Additionally, tumors from the 3-MPA-treated mice had decreased β-catenin expression (Fig. 5H). Together, these data corroborate the in vitro reports that 3-MPA had antitumor effects in vivo by inhibiting Wnt/β-catenin signaling.

4. Discussion

OS is the most common and deadly type of bone cancer in both adults and children [19,20]. Recently, efforts to successfully treat OS have stagnated due to the lack of effective therapeutic targets [21], emphasizing the importance of identifying novel biomarkers to improve the treatment of OS [22].

The burgeoning field of ‘‘cancer neuroscience’’, which focuses on studying cancer-nervous system interactions [23], provides a new perspective on tumor therapy, including that of OS. According to prior research, tumor cells utilize the neurotransmitter-initiated signaling pathway to promote unregulated growth and metastasis [16,24]. GABA is conventionally viewed as the major inhibitory neurotransmitter in the CNS. In recent years, GABA was found to be an essential component regulating major malignant phenotypes of human tumors in the TME [11,13,16,25]. Intriguingly, GABA-positive tumors express high levels of GAD1 [13], which is a rate-limiting enzyme in GABA synthesis [15]. Notably, GAD1 expression is mainly restricted to the CNS [11]. A body of data suggests that targeting GAD1 may be a novel therapeutic strategy [9,11,13,15], but its expression status and functional mechanisms in OS remain unclear.

In our research, GAD1 expression was observed to be significantly elevated in OS clinical samples compared with adjacent normal bone tissues. Consistent with our findings, high GAD1 is related to advanced tumor status and is associated with poor prognosis in several kinds of tumors [26–29]. In addition, GAD1 was overexpressed in OS-derived cells compared to human osteoblast cells (hFoB1.19). These findings suggest that GAD1, a GABAergic neuronal marker, could contribute to OS development as an oncogene.

Treatment with 3-MPA was reported to block GABA synthesis via GAD1 inhibition [30] and suppress lung and colorectal cancer cell proliferation [11] and oral cancer cell migration [15]. As increased GAD1 levels were observed in OS clinical samples and 3-MPA exerted antitumor effects in other solid tumors, we next used 3-MPA to evaluate the antiproliferative effects on HOS and MG-63 cells. Using colony formation and cell viability experiments, we discovered that 3-MPA inhibits OS cell viability by promoting cell cycle arrest. Further subcutaneous xenograft models confirmed the antitumor efficacy of 3-MPA in vivo. In a previous study, Kimura, Ryota

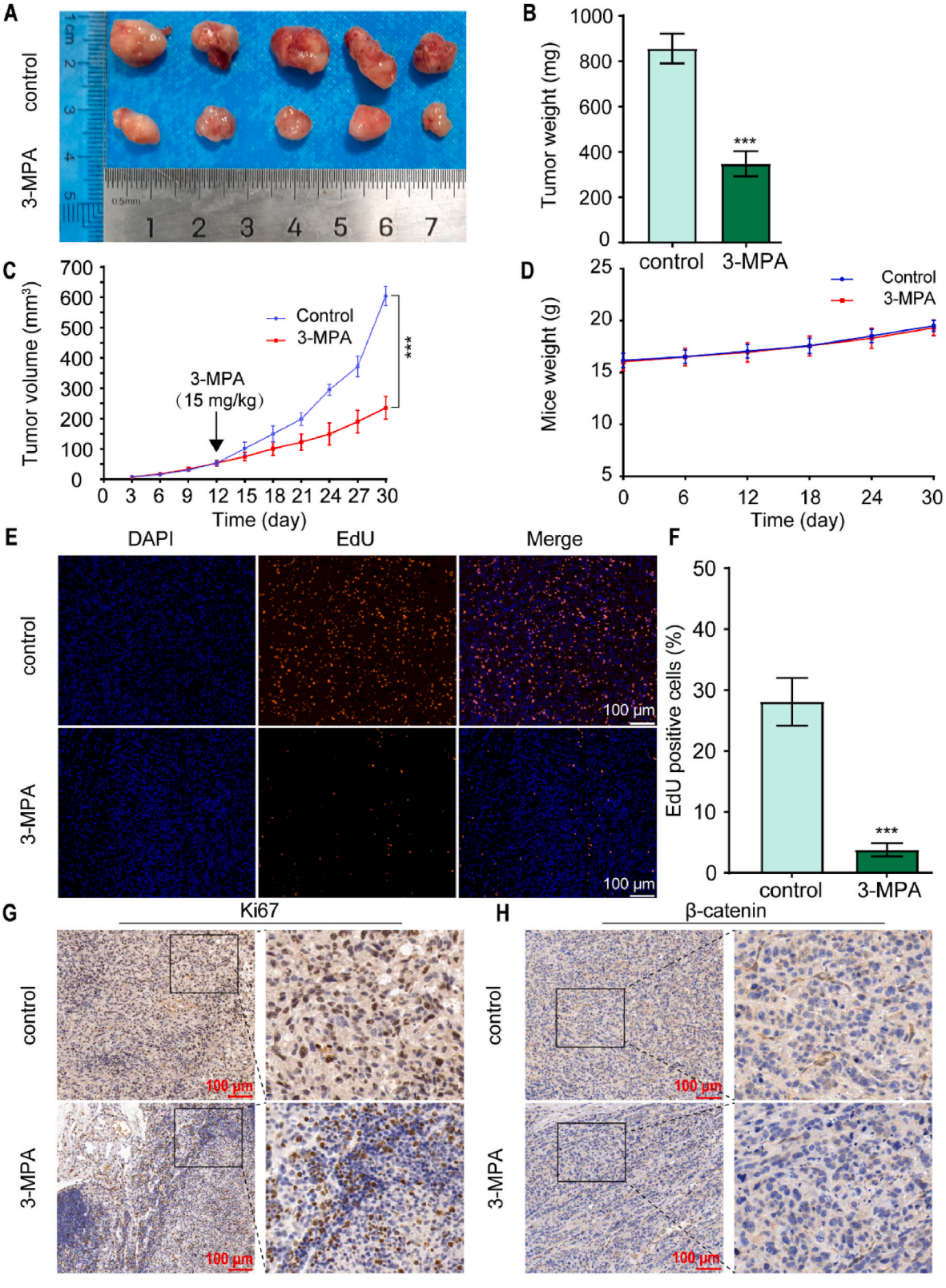

(caption on next page)

Fig. 5. Treatment with 3-MPA inhibits the development of subcutaneously implanted HOS tumors. (A) Representative images show smaller tumors in the 3-MPA-treated groups compared to the control groups. (B) Average weight of the tumor obtained on the final day of the trial. (C) Tumor volume was calculated throughout the therapy duration. (D) Mouse weights throughout the course of the study. (The data are given in the form of the mean ± SD; n = 5, $^{***}p < 0.001$). (E) Representative images showing that tumors of the control group exhibited more EdU-positive cells than those of the 3-MPA-treated group, EdU (red), DAPI (blue). (F) Quantitative data of EdU-positive cells in the two groups ($^{***}p < 0.001$). (G–H) Images of Ki67 and β-catenin immunohistochemical staining in tumor samples. The scale bars are 100 μm.

et al. reported that 3-MPA treatment could reduce the migration and invasion ability of human oral cancer cells [15]. However, our findings indicated that 3-MPA did not have an impact on the migration and invasion of OS cells. Additionally, there was no alteration in the protein expression level of EMT markers. This may be due to different types of cancer, or it may be that a higher concentration of 3-MPA is required to affect the migration and invasion ability of OS cells, which requires further research. The Wnt/β-catenin signaling pathway is among the most important cascades that regulate cellular development and differentiation [31]. Under normal physiological conditions, this signaling pathway is tightly controlled, and dysregulation of the Wnt/β-catenin signaling pathway is frequently connected to tumor formation or relapse [32,33]. Several findings show that abnormal stimulation of this signaling pathway has a crucial function in tumorigenicity in addition to metastatic dissemination in OS patients [34,35]. In our research, we found that 3-MPA therapy inhibited β-catenin expression and its direct target gene cyclin D1 in a concentration-dependent manner in OS cells. Furthermore, treatment with 3-MPA suppressed the growth of HOS tumors in nude mice, and tumors from the 3-MPA-treated mice exhibited reduced β-catenin and Ki67 expression. As β-catenin signaling, a critical downstream controller of Wnt signaling, is known to be oncogenic in numerous contexts [18], these data imply that the inactivation of β-catenin is the mechanism by which 3-MPA inhibits the growth of OS. Our results are consistent with previous studies. Kimura R et al. suggested that the expression of GAD1 controls the localization of β-catenin [15]. Huang et al. suggested that the upregulation of GAD1 in tumor cells leads to enhanced β-catenin signaling through the generation of GABA, which activates GABAB receptors [11]. Li CM et al. suggested that GAD1 may be a target gene of β-catenin in tumor tissues [36], indicating the potential existence of a positive feedback loop between the expression of GAD1 and β-catenin activation. However, the mechanism of interaction between GAD1 and β-catenin remains unclear, and more research is needed in the future.

Our research also had several limitations. The mechanism by which OS acquires the GABAergic neuronal marker gene GAD1 remains unclear. Furthermore, the application of 3-MPA is still in the experimental exploration stage, and further research is needed to determine its potential clinical implications. We have only provided preliminary insights into the impact of 3-MPA on the Wnt/β-catenin signaling pathway, and more protein alterations in the Wnt/β-catenin signaling pathway following GAD1 inhibition require further investigation. Additionally, we did not establish a subcutaneous xenograft model using MG-63 cells, and the effect of 3-MPA on the tumor growth of MG-63 cells in vivo remains unknown. We will address these limitations and incorporate them into our future studies to further improve the comprehensiveness of our research.

5. Conclusions

In summary, we herein found that OS displays increased expression of the GABAergic neuronal marker GAD1. The inhibitor 3-MPA can suppress OS tumor growth by inhibiting Wnt/β-catenin. Inhibiting GAD1 may be a novel therapeutic strategy for OS patients.

Ethics statement

The use of human specimens in this study was approved by the Ethics Committee of the First Affiliated Hospital of Chongqing Medical University, with approval number 2021-175. The animal experiment in this study was approved by the Ethics Committee of the First Affiliated Hospital of Chongqing Medical University, with approval number 2022-K285.

Funding statement

This research was funded by National Natural Science Foundation of China (No. 82172682), Chongqing Science & Technology Commission (No. CSTB2023NSCQ-MSX0472), and the Clinical Medical College of North Sichuan Medical College - Affiliated Hospital Research and Development Plan Project: 2023-2GC003.

Data availability statement

The original findings of this study are included in the article. Any additional inquiries can be directed to the corresponding author.

CRediT authorship contribution statement

Changchun Jian: Writing – review & editing, Writing – original draft, Methodology, Data curation, Conceptualization. **Ben Wang:** Software, Conceptualization. **Hai Mou:** Validation, Methodology, Conceptualization. **Ye Zhang:** Writing – original draft, Methodology, Conceptualization. **Chaohua Yang:** Data curation. **Qiu Huang:** Data curation. **Yunsheng Ou:** Writing – review & editing, Supervision, Conceptualization.

Declaration of competing interest

The authors declare that they have no known competing financial interests or personal relationships that could have appeared to influence the work reported in this paper.

Appendix A. Supplementary data

Supplementary data to this article can be found online at https://doi.org/10.1016/j.heliyon.2024.e31444.

References

[1] Z. Hu, et al., Current status and prospects of targeted therapy for osteosarcoma, Cells 11 (21) (2022).
[2] P.S. Meltzer, L.J. Helman, New horizons in the treatment of osteosarcoma, N. Engl. J. Med. 385 (22) (2021) 2066–2076.
[3] E.N. Arner, J.C. Rathmell, Metabolic programming and immune suppression in the tumor microenvironment, Cancer Cell 41 (3) (2023) 421–433.
[4] S.R. Ali, et al., Nerve density and neuronal biomarkers in cancer, Cancers 14 (19) (2022).
[5] R. Takahashi, H. Ijichi, M. Fujishiro, The role of neural signaling in the pancreatic cancer microenvironment, Cancers 14 (17) (2022).
[6] C. Magnon, et al., Autonomic nerve development contributes to prostate cancer progression, Science 341 (6142) (2013) 1236361.
[7] Y. Hayakawa, et al., Nerve growth factor promotes gastric tumorigenesis through aberrant cholinergic signaling, Cancer Cell 31 (1) (2017) 21–34.
[8] B.W. Renz, et al., Cholinergic signaling via muscarinic receptors directly and indirectly suppresses pancreatic tumorigenesis and cancer stemness, Cancer Discov. 8 (11) (2018) 1458–1473.
[9] P.M. Schnepp, et al., GAD1 upregulation programs aggressive features of cancer cell metabolism in the brain metastatic microenvironment, Cancer Res. 77 (11) (2017) 2844–2856.
[10] E. Wingrove, et al., Transcriptomic hallmarks of tumor plasticity and stromal interactions in brain metastasis, Cell Rep. 27 (4) (2019) 1277–1292.e7.
[11] Huang, et al., Cancer-cell-derived GABA promotes beta-catenin-mediated tumour growth and immunosuppression, Nat. Cell Biol. 24 (2) (2022) 230–241.
[12] A. Takehara, et al., Gamma-aminobutyric acid (GABA) stimulates pancreatic cancer growth through overexpressing GABAA receptor pi subunit, Cancer Res. 67 (20) (2007) 9704–9712.
[13] D. Huang, et al., GABAergic signaling beyond synapses: an emerging target for cancer therapy, Trends Cell Biol. 33 (5) (2023) 403–412.
[14] A. Opolski, et al., The role of GABA-ergic system in human mammary gland pathology and in growth of transplantable murine mammary cancer, J. Exp. Clin. Cancer Res. 19 (3) (2000) 383–390.
[15] R. Kimura, et al., Glutamate acid decarboxylase 1 promotes metastasis of human oral cancer by β-catenin translocation and MMP7 activation, BMC Cancer 13 (2013) 555.
[16] S.H. Jiang, et al., Neurotransmitters: emerging targets in cancer, Oncogene 39 (3) (2020) 503–515.
[17] T.Z. Veres, et al., Dendritic cell-nerve clusters are sites of T cell proliferation in allergic airway inflammation, Am. J. Pathol. 174 (3) (2009) 808–817.
[18] T. Zhan, N. Rindtorff, M. Boutros, Wnt signaling in cancer, Oncogene 36 (11) (2017) 1461–1473.
[19] G.N. Yan, Y.F. Lv, Q.N. Guo, Advances in osteosarcoma stem cell research and opportunities for novel therapeutic targets, Cancer Lett. 370 (2) (2016) 268–274.
[20] P.M. Dana, et al., Molecular signaling pathways as potential therapeutic targets in osteosarcoma, Curr. Med. Chem. 29 (25) (2022) 4436–4444.
[21] S. Smeland, et al., Survival and prognosis with osteosarcoma: outcomes in more than 2000 patients in the EURAMOS-1 (European and American Osteosarcoma Study) cohort, Eur. J. Cancer 109 (2019) 36–50.
[22] B. Celik, et al., Regulation of molecular targets in osteosarcoma treatment, Int. J. Mol. Sci. 23 (20) (2022).
[23] M. Monje, et al., Roadmap for the emerging field of cancer neuroscience, Cell 181 (2) (2020) 219–222.
[24] B. Zhang, et al., B cell-derived GABA elicits IL-10(+) macrophages to limit anti-tumour immunity, Nature 599 (7885) (2021) 471–476.
[25] S.Z. Young, A. Bordey, GABA's control of stem and cancer cell proliferation in adult neural and peripheral niches, Physiology 24 (2009) 171–185.
[26] Y.Y. Lee, et al., Glutamate decarboxylase 1 overexpression as a poor prognostic factor in patients with nasopharyngeal carcinoma, J. Cancer 7 (12) (2016) 1716–1723.
[27] S. Soejima, et al., GAD1 expression and its methylation as indicators of malignant behavior in thymic epithelial tumors, Oncol. Lett. 21 (6) (2021) 483.
[28] M. Tsuboi, et al., Prognostic significance of GAD1 overexpression in patients with resected lung adenocarcinoma, Cancer Med. 8 (9) (2019) 4189–4199.
[29] H. Yan, et al., DNA methylation reactivates GAD1 expression in cancer by preventing CTCF-mediated polycomb repressive complex 2 recruitment, Oncogene 35 (30) (2016) 3995–4008.
[30] K. Sasaki, et al., Effects of bilobalide on gamma-aminobutyric acid levels and glutamic acid decarboxylase in mouse brain, Eur. J. Pharmacol. 367 (2–3) (1999) 165–173.
[31] B. Taciak, et al., Wnt signaling pathway in development and cancer, J. Physiol. Pharmacol. 69 (2) (2018).
[32] Y. Duchartre, Y.M. Kim, M. Kahn, The Wnt signaling pathway in cancer, Crit. Rev. Oncol. Hematol. 99 (2016) 141–149.
[33] D. Tai, et al., Targeting the WNT signaling pathway in cancer therapeutics, Oncol. 20 (10) (2015) 1189–1198.
[34] C. Chen, et al., Aberrant activation of Wnt/β-catenin signaling drives proliferation of bone sarcoma cells, Oncotarget 6 (19) (2015) 17570–17583.
[35] G. Danieau, et al., New insights about the wnt/β-catenin signaling pathway in primary bone tumors and their microenvironment: a promising target to develop therapeutic strategies? Int. J. Mol. Sci. 20 (15) (2019).
[36] C.M. Li, et al., CTNNB1 mutations and overexpression of Wnt/beta-catenin target genes in WT1-mutant Wilms' tumors, Am. J. Pathol. 165 (6) (2004) 1943–1953.